TECHNICAL RESEARCH REPORT

SYSTEMS RESEARCH CENTER

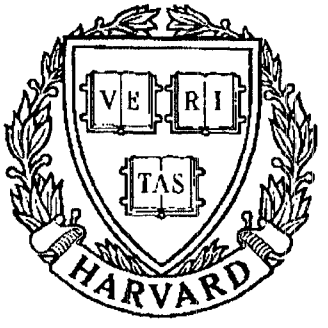

Supported by the National Science Foundation Engineering Research Center Program (NSFD CD 8803012), the University of Maryland, Harvard University, and Industry

Steady Rigid-Body Motions in a Central Gravitational Field

by L.-S. Wang, J.H. Maddocks and P.S. Krishnaprasad

TR 91-50

STEADY RIGID-BODY MOTIONS IN A CENTRAL GRAVITATIONAL FIELD

Li-Sheng Wang * J.H. Maddocks* P.S. Krishnaprasad †

ABSTRACT.

In recent work, the exact dynamic equations for the motion of a finite rigid body in a central gravitational field were shown to be of Hamiltonian form with a noncanonical structure. In this paper, the notion of relative equilibrium is introduced based upon this exact model. In relative equilibrium, the orbit of the center of mass of the rigid body is a circle, but the center of attraction may or may not lie at the center of the orbit. This feature is used to classify *great-circle* and *non-great-circle* orbits. The existence of non-great-circle relative equilibria for the exact model is proved from various variational principles. While the orbital offset of the non-great-circle solutions is necessarily small, a numerical study reveals that there can be significant changes in orientation away from the classic Lagrange relative equilibria, which are solutions of an approximate model.

1. Introduction

This paper describes some results concerning the relative equilibria, or steady circular orbits, of a rigid body of finite extent moving under the effects of an inverse square gravitational force field. In different parameter regimes, the analysis applies equally well

This work was supported in part by the Grants AFOSR-URI-87-0073, AFOSR-89-0376, NSFD-CDR-08803012, and by an account at the San Diego Super-Computer Center.

* Mathematics Department, University of Maryland, College Park, MD 20742.

† Electrical Engineering Department & Systems Research Center, University of Maryland, College Park, MD 20742.

to an artificial satellite orbiting the Earth, to a moon orbiting a planet, or to a planet orbiting a sun. In any of these cases the approximate problem at hand is that of the motion of a two-body system. We shall further assume that a restricted two body problem is appropriate, i.e. one of the bodies is extremely massive in comparison to the other, so that the motion of the heavier body is unaffected by the motion of the lighter one.

Of course if the two bodies are further approximated as two point masses the restricted two body problem is completely integrable and is completely solved. The points of interest that will be addressed here arise due to effects arising from the finite extent of the bodies. This topic has also received considerable attention, for example the n-rigid-body problem studied in [5], the three-rigid-body problem discussed in [6], [3], and the effects of finite extent of bodies on the equilibria of the restricted three-rigid-body problem described in [7]. For the two-rigid-body problem and the restricted two-rigid-body problem, there are extensive discussions in [2], and in [23], [26], [12], and [22] where problems including gyrostats are considered. Moreover, the steady-state (rotational) motions (or relative equilibria) of a rigid body in a central gravity field and their stability were considered in [24], [21], [11], [14], and [1]. Similar problems are studied in [31] for interconnected gyrostats. All of the above analyses make some approximation of the gravitational force acting on the rigid body. We shall show that for some rigid bodies, steady-state motions of the *exact* problem are qualitatively, and quantitatively different from the classical so-called *Lagrange* or *regular motions* in which one of the principal axes coincides with the radius vector. The precise differences are further described below.

Approximation of a finite rigid body as a point mass can be justified in two distinct ways. A point mass is an exact model in the case of a rigid body having spherical mass distribution (a result due to Newton). Alternatively, approximation as a point mass appears to be reasonable if a body is very small in comparison to a typical orbit radius. In the case of an Earth-satellite system, the justification for treating the Earth as a point mass is approximate spherical symmetry, and the justification for treating the satellite as a point mass is that it is very small. Deviations of the Earth from spherical symmetry are an important effect in low Earth orbits, and the problem has been studied by many workers including recent work of Deprit and collaborators [4]. Here we are concerned with

effects associated with the approximation of the satellite as a point mass. Accordingly we shall hereafter assume the Earth to be exactly spherical, and therefore exactly equivalent to (an extremely heavy) point mass.

The equations of motion for the restricted two body problem comprise a force balance equation, and a moment balance equation. A typical line of analysis, apparently tracing back to Lagrange, and followed by Beletskii [2], Sarychev [25] and Roberson [22] among others, is to retain the lowest-order nonvanishing term of the potential in each equation. As a consequence of this strategy the force balance equation involves only the zeroth order term of the potential. Moreover the force balance equations decouple from the moment balance equations to give force conditions that are identical with those of a point mass. The steady-state solutions, or relative equilibria, are circular orbits that are also *great circles* in the sense that the center of the circular orbit coincides with the center of the Earth. Once the orbits have been determined, the moment balance equation must still be satisfied. In the moment balance the first nonvanishing term of the potential is of second-order. It may then be concluded that the satellite must be oriented such that its principal axes of inertia are aligned with the radius, tangent and normal vectors to the circular orbit. When signs are associated with the principal axes there are $(6 \times 4 =)$ 24 such orientations depending upon whether it is the axis with largest inertia that is tangent etc. Some of these solutions are known to be stable, some are known to be unstable, and the nonlinear stability properties of others are indeterminate.

In a recent work [29], the above problem has been reanalyzed from the viewpoint of Hamiltonian mechanics. In particular it was shown that the evolution equations can be written as a (noncanonical) Hamiltonian system with the potential being one term in the Hamiltonian. Different approximations of the potential then provide different dynamical systems that can be analyzed. In the case of a second-order approximation of the potential the classic results described above were recovered, albeit by a different, more consistent, approximation scheme. Interestingly in the analysis of the second-order model considerable effort had to be spent to exclude the possibility of *non-great-circle* relative equilibria in which the orbit vector sweeps out a cone rather than a disk. The possibility of non-great-circle solutions is excluded *a priori* in the approximations adopted by most previous

authors. In light of this experience we proceeded to consider the exact problem in which the potential is not approximated, and in this paper we shall show that great-circle equilibria are exceptional (i.e. non-generic) for bodies without planes of symmetry. Moreover any body with no great-circle solutions has at least *four* non-great-circle steady orbits. On the other hand in the *exact* problem for a body with three planes of symmetry (as is implicitly assumed in the second-order model) there are *at least* 24 great-circle solutions.

The counterintuitive result concerning existence of non-great-circle solutions can best be explained by the observation that as far as an inverse square gravitational field is concerned, the center of mass of a body is not a distinguished point. However it is physically clear that the lateral displacement of the plane of the orbit of the center of mass is necessarily very small, and in particular smaller than the dimension of the satellite. Nevertheless we will present numerical examples which show that this tiny offset in orbit can be associated with a large rotation away from the classic 24 orientations predicted by the second-order model. Consequently these non-great-circle relative equilibria may be of importance in the understanding and design of Earth pointing satellites. In particular, we argue that large deviations in orientation are to be expected when two or more principal inertias are nearly equal.

In [2], [26], [21] and [1], non-great-circle relative equilibria (sometimes called *oblique regular motions*) have already been discussed. Their approaches were based on various approximate models of the potential which used local coordinates such as Euler angles. Here, we are dealing with an exact Hamiltonian model. The work most closely related is [1] in which it was assumed that the ratio between the body size and the radius is very small and only oblique regular motions close to the *regular motions* (i.e. to the great-circle relative equilibria) are observed. Nevertheless, we have verified numerically that large deviations in orientation from these classic motions are possible. In fact, we exhibit large changes of orientation for a particularly simple idealized rigid body which we call a molecule, namely six point masses, two lying on each principal axis. In order to magnify the effects of higher order terms in approximation of the potential function (cf. [14]), the three moments of inertia are chosen to be close to each other. On the other hand, the mass distribution of the molecule is designed to be as asymmetric as

possible to emphasize the orientation change. During the numerical search for the relative equilibria of such structures, continuation methods are adopted to solve efficiently the appropriate system of nonlinear algebraic equations by successive application of Newton-Raphson iterations. We also apply an error analysis (due to Kantorovich) which guarantees that exact solutions exist close to our numerical approximations. The error analysis is particularly important because the problems turn out to be severely ill-conditioned in the appropriate parameter regimes. Indeed in order to obtain sufficient accuracy to guarantee a solution, we implemented our algorithm in double-precision on a 96-bit machine (actually in Fortran on a CRAY which leads to approximately 29 significant digits). The numerical non-great-circle relative equilibria we found justify the statement that while the orbital offset is very small, the change in orientation from the regular motions can be significant.

2. Dynamic Equations and Non-dimensionalization

We consider the motion of a rigid body $\mathcal{B}^*$ moving in a central inverse-square gravitational force field that is generated by a massive body $\mathcal{B}_0{}^*$. The body $\mathcal{B}_0{}^*$ is assumed to be stationary so that a restricted two-body problem is at hand. A configuration of the system is depicted in Figure 2.1. We assume that the reference or inertial frame is located at the center O of the inverse square field due to the mass of $\mathcal{B}_0{}^*$. Let C denote the center of mass of the moving body $\mathcal{B}^*$, and let r^* denote the vector from O to C in the inertial frame. The attitude of the rigid body $\mathcal{B}^*$ is described by a set of orthogonal basis vectors located at C and fixed relative to $\mathcal{B}^*$, which will be termed the *body frame*. Let the orientation transformation from the body frame to the inertial frame be denoted by B, which is a rotation matrix or element of the special orthogonal group $SO(3)$. By elementary analysis, the time derivative of the rotation matrix can be written as

$$\dot{B} \;=\; B\widehat{\Omega^*}, \tag{2.1}$$

where $\widehat{\ }$ maps the instantaneous angular velocity $\Omega^* \in \mathbb{R}^3$ of B (or $\mathcal{B}^*$) in the body frame, to an element in $so(3)$, the space of 3×3 skew-symmetric matrices, according to the rule

$$\begin{pmatrix} \widehat{\Omega^*_1} \\ \Omega^*_2 \\ \Omega^*_3 \end{pmatrix} = \begin{pmatrix} 0 & -\Omega^*_3 & \Omega^*_2 \\ \Omega^*_3 & 0 & -\Omega^*_1 \\ -\Omega^*_2 & \Omega^*_1 & 0 \end{pmatrix}. \tag{2.2}$$

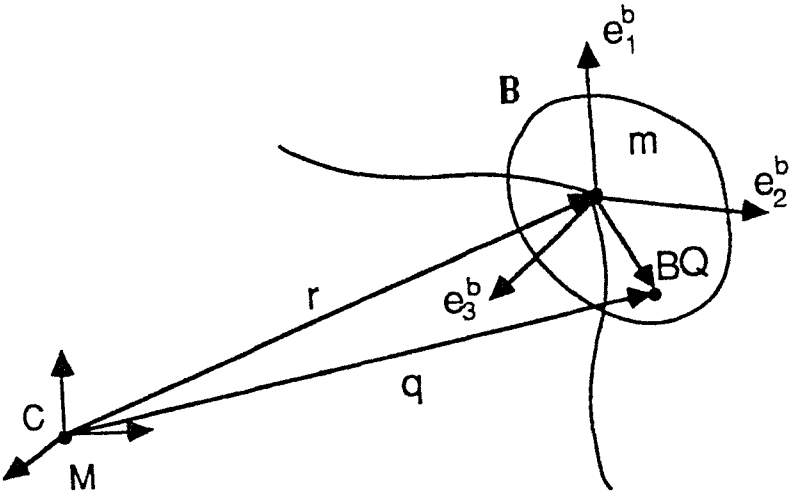

Figure 2.1. A Rigid Body in a Central Gravitational Field

In (2.1) and what follows, we adopt the convention that variables with an asterisk * have dimension, and the dot operator $\dot{}$ denotes the derivative of the corresponding variable with respect to the dimensional time variable t^*.

Let Q^* be the vector from C to an arbitrary material point in $\mathcal{B}^*$ relative to the body frame, and denote the associated mass element by $dm(Q^*)$. Then the linear momentum of $\mathcal{B}^*$ can be written as

$$p^* = \int_{\mathcal{B}^*} \frac{d}{dt}(r^* + BQ^*)\, dm(Q^*) = m\dot{r^*}, \tag{2.3}$$

where m is the total mass of $\mathcal{B}^*$. Here the fact that $\int_{\mathcal{B}^*} Q^* dm(Q^*) = 0$ has been used. On the other hand, the angular momentum of $\mathcal{B}^*$ about O (expressed in the inertial frame) is

$$\begin{aligned} \pi^* &= \int_{\mathcal{B}^*} (r^* + BQ^*) \times \frac{d}{dt}(r^* + BQ^*)\, dm(Q^*) \\ &= r^* \times m\dot{r^*} + B\mathbf{I}^*\Omega^*, \end{aligned} \tag{2.4}$$

where

$$\mathbf{I}^* = \int_{\mathcal{B}^*} \widehat{Q^*}\widehat{Q^*}^T \, dm(Q^*) \tag{2.5}$$

is the *moment of inertia* of $\mathcal{B}^*$ relative to the body frame.

The gravitational force exerted on $\mathcal{B}^*$ by $\mathcal{B}_0{}^*$ can be derived from the potential

$$V = -\int_{\mathcal{B}_0{}^*} \int_{\mathcal{B}^*} \frac{G}{|q^* - (r^* + BQ^*)|} \, dm(Q^*) dm_0(q^*), \tag{2.6}$$

where G is the universal gravitational constant, and q^* is a vector from O to a material point in $\mathcal{B}_0{}^*$ with mass $dm_0(q^*)$. Now we assume that the body $\mathcal{B}_0{}^*$ has spherical symmetry. Then by elementary analysis it can be shown that the potential function V simplifies to

$$V = -\int_{\mathcal{B}^*} \frac{GM}{|r^* + BQ^*|} \, dm(Q^*), \tag{2.7}$$

where M is the total mass of the body $\mathcal{B}_0{}^*$. Consequently, assuming there are no forces external to the two-body system, the resultant force on $\mathcal{B}^*$ can be expressed as

$$f = -\int_{\mathcal{B}^*} \frac{GM(r^* + BQ^*)}{|r^* + BQ^*|^3} \, dm(Q^*). \tag{2.8}$$

Similarly, assuming there is no external couple acting on $\mathcal{B}^*$, the resultant torque is

$$\tau = -\int_{\mathcal{B}^*} (r^* + BQ^*) \times \frac{GM(r^* + BQ^*)}{|r^* + BQ^*|^3} \, dm(Q^*) = 0. \tag{2.9}$$

Balance of linear momentum then implies, from (2.3), and (2.8),

$$\dot{p^*} = -\int_{\mathcal{B}^*} \frac{GM(r^* + BQ^*)}{|r^* + BQ^*|^3} \, dm(Q^*). \tag{2.10}$$

On the other hand, balance of angular momentum implies

$$\dot{\pi^*} = 0. \tag{2.11}$$

Let $\Pi^* = \mathbf{I}^*\Omega^*$ denote the instantaneous body angular momentum of $\mathcal{B}^*$. Then from (2.1), (2.4), and (2.9), we can derive an evolution equation for Π^*

$$\dot{\Pi^*} = \Pi^* \times \mathbf{I}^{*-1}\Pi^* + \int_{\mathcal{B}^*} \frac{GM(B^T r^* \times Q^*)}{|r^* + BQ^*|^3} \, dm(Q^*). \tag{2.12}$$

Consequently, equations (2.1), (2.3), (2.10), (2.12) completely describe the motion of the rigid body $\mathcal{B}^*$ moving in the gravitational force field.

Now we define convected or body variables,

$$\lambda^* = B^T r^*, \qquad \mu^* = B^T p^*,$$

which are vectors expressed in coordinates with respect to the moving body frame. In terms of these variables, the equations of motion may be written as

$$\dot{\Pi}^* = \Pi^* \times \mathbf{I}^{*-1}\Pi^* + \int_{\mathcal{B}^*} \frac{GM(\lambda^* \times Q^*)}{|\lambda^* + Q^*|^3}\, dm(Q^*), \tag{2.13a}$$

$$\dot{\lambda}^* = \lambda^* \times \mathbf{I}^{*-1}\Pi^* + \mu^*/m, \tag{2.13b}$$

$$\dot{\mu}^* = \mu^* \times \mathbf{I}^{*-1}\Pi^* - \int_{\mathcal{B}^*} \frac{GM(\lambda^* + Q^*)}{|\lambda^* + Q^*|^3}\, dm(Q^*), \tag{2.13c}$$

$$\dot{B} = B\widehat{\mathbf{I}^{*-1}\Pi^*}. \tag{2.13d}$$

We now nondimensionalize this system. With mass, length, and time scales,

$$m, \qquad l = \left(\frac{tr(\mathbf{I}^*)}{m}\right)^{\frac{1}{2}}, \qquad \text{and} \quad T = \left(\frac{l^3}{GM}\right)^{\frac{1}{2}}, \tag{2.14}$$

the nondimensional variables are

$$\lambda = \frac{\lambda^*}{l}, \quad \mu = \frac{\mu^*}{mlT^{-1}}, \quad \Pi = \frac{\Pi^*}{ml^2T^{-1}}, \quad \text{and} \quad t = \frac{t^*}{T}. \tag{2.15}$$

Next we introduce a nondimensional body (or domain of integration) $\mathcal{B}$. From the dimensional mass measure dm, we define

$$Q = \frac{Q^*}{l}, \qquad d\nu(Q) = \frac{1}{m} dm(Q^*), \tag{2.16}$$

and accordingly,

$$\int_{\mathcal{B}} d\nu(Q) = \int_{\mathcal{B}^*} \frac{1}{m} dm(Q^*) = 1. \tag{2.17}$$

The nondimensional moment of inertia of $\mathcal{B}$ is

$$\mathbf{I} = \frac{\mathbf{I}^*}{tr(\mathbf{I}^*)}, \tag{2.18}$$

so that

$$tr(\mathbf{I}) \;=\; 1. \qquad (2.19)$$

In terms of these nondimensional variables, the dynamical equations (2.13) can be expressed as

$$\Pi' \;=\; \Pi \times \mathbf{I}^{-1}\Pi \;+\; \int_{\mathcal{B}} \frac{\lambda \;\times\; Q}{|\lambda \;+\; Q|^3}\, d\nu(Q), \qquad (2.20a)$$

$$\lambda' \;=\; \lambda \times \mathbf{I}^{-1}\Pi \;+\; \mu, \qquad (2.20b)$$

$$\mu' \;=\; \mu \times \mathbf{I}^{-1}\Pi \;-\; \int_{\mathcal{B}} \frac{\lambda \;+\; Q}{|\lambda \;+\; Q|^3}\, d\nu(Q), \qquad (2.20c)$$

$$B' \;=\; B\widehat{\mathbf{I}^{-1}\Pi}. \qquad (2.20d)$$

where the prime $'$ denotes a derivative with respect to the nondimensional time t. It is the nondimensional system (2.20) that will be investigated in the following Sections.

3. Relative Equilibria

Equations (2.20 a,b,c) do not include the attitude B and are therefore decoupled from (2.20d). Accordingly, the equations of motion (2.20 a,b,c) on the nine dimensional space $(\Pi, \lambda, \mu) \in \mathbb{R}^9$ will be called the *reduced dynamics*. Equilibria of the reduced dynamics give rise to motions in the original space (r^*, B, p^*, Π^*) satisfying (2.1), (2.3), (2.10), (2.12) such that the rigid body $\mathcal{B}^*$ exhibits a steady spin about the fixed center O, while the center of mass C moves in a circular orbit. Such a motion will be referred to as a *relative equilibrium*. All such motions are equilibria relative to a steadily rotating frame. There is no a priori reason that the center of the circular orbit traced by C need coincide with the origin O. Indeed we will exhibit relative equilibria where O is not the center of the orbit.

Conditions of relative equilibria are easily found from the reduced dynamics. In terms of the reduced variables, we have the following equations,

$$\Pi \times \mathbf{I}^{-1}\Pi \;+\; \int_{\mathcal{B}} \frac{\lambda \;\times\; Q}{|\lambda \;+\; Q|^3}\, d\nu(Q) \;=\; 0, \qquad (3.1a)$$

$$\lambda \times \mathbf{I}^{-1}\Pi + \mu = 0, \tag{3.1b}$$

$$\mu \times \mathbf{I}^{-1}\Pi - \int_{\mathcal{B}} \frac{\lambda + Q}{|\lambda + Q|^3}\, d\nu(Q) = 0. \tag{3.1c}$$

Discussion of the existence of solutions to (3.1), and their qualitative and quantitative features are the main theme of this paper.

In [29], a Hamiltonian approach to this problem was exploited. It was shown that the reduced dynamics (2.20 a, b, c) can be written as a Hamiltonian system

$$\frac{d}{dt}\begin{pmatrix} \Pi \\ \lambda \\ \mu \end{pmatrix} = \Lambda\, \nabla H. \tag{3.2}$$

with Hamiltonian

$$H(\Pi, \lambda, \mu) = \frac{1}{2} < \Pi, \mathbf{I}^{-1}\Pi > + \frac{|\mu|^2}{2} - \int_{\mathcal{B}} \frac{1}{|\lambda + Q|}\, d\nu(Q), \tag{3.3}$$

and Poisson tensor,

$$\Lambda = \begin{pmatrix} \hat{\Pi} & \hat{\lambda} & \hat{\mu} \\ \hat{\lambda} & 0 & \mathbf{1} \\ \hat{\mu} & -\mathbf{1} & 0 \end{pmatrix}, \tag{3.4}$$

which is a 9×9 skew-symmetric matrix with block structure. Here the notation $\hat{}$ is defined through (2.2), and $\mathbf{1}$ denotes the 3×3 identity matrix. The Poisson tensor Λ is rank-degenerate. In fact, its null space is one-dimensional and is spanned by the vector

$$\nabla C(\Pi, \lambda, \mu) = \begin{pmatrix} \Pi + \lambda \times \mu \\ \mu \times (\Pi + \lambda \times \mu) \\ (\Pi + \lambda \times \mu) \times \lambda \end{pmatrix}, \tag{3.5}$$

where C is the total angular momentum,

$$C(\Pi, \lambda, \mu) = \frac{1}{2}\,|\Pi + \lambda \times \mu|^2. \tag{3.6}$$

The function C is sometimes called a *Casimir* function of the noncanonical Hamiltonian structure, cf. [9]. It is clear from (3.2) that at relative equilibria, the vector ∇H must lie in the null space of Λ, in other words,

$$\nabla H(\Pi, \lambda, \mu) = \zeta\, \nabla C(\Pi, \lambda, \mu), \tag{3.7}$$

for some scalar ζ. Accordingly, there is a variational principle which characterizes the relative equilibria, namely

$$\begin{aligned} &\textit{make stationary} \qquad H(\Pi,\ \lambda,\ \mu) \\ &\textit{subject to the constraint}\ \ C(\Pi,\ \lambda,\ \mu)\ =\ \text{constant}. \end{aligned} \tag{3.8}$$

The first-order conditions for (3.8) are nothing other than (3.7), which can also be expressed as

$$\begin{pmatrix} \mathbf{I}^{-1}\Pi \\ \nabla_\lambda \tilde{V}(\lambda) \\ \mu \end{pmatrix} \ =\ \zeta \begin{pmatrix} \Pi + \lambda \times \mu \\ \mu \times (\Pi + \lambda \times \mu) \\ (\Pi + \lambda \times \mu) \times \lambda \end{pmatrix}, \tag{3.9}$$

where

$$\tilde{V}(\lambda)\ =\ -\int_{\mathcal{B}} \frac{1}{|\lambda\ +\ Q|}\, dm(Q). \tag{3.10}$$

Equation (3.9) can be immediately simplified to

$$\begin{pmatrix} \mathbf{I}^{-1}\Pi \\ \nabla_\lambda \tilde{V}(\lambda) \\ \mu \end{pmatrix} \ =\ \begin{pmatrix} \zeta(\Pi + \lambda \times \mu) \\ \mu \times \mathbf{I}^{-1}\Pi \\ \mathbf{I}^{-1}\Pi \times \lambda \end{pmatrix}. \tag{3.11}$$

Thus μ can be eliminated from (3.11) to yield

$$\begin{pmatrix} \mathbf{I}^{-1}\Pi \\ \nabla_\lambda \tilde{V}(\lambda) \end{pmatrix} \ =\ \begin{pmatrix} \zeta(\Pi + \lambda \times (\mathbf{I}^{-1}\Pi \times \lambda)) \\ (\mathbf{I}^{-1}\Pi \times \lambda) \times \mathbf{I}^{-1}\Pi \end{pmatrix}. \tag{3.12}$$

By introducing the body angular velocity $\Omega = \mathbf{I}^{-1}\Pi$, we find

$$\begin{aligned} \mathbf{I}\Omega + \lambda \times (\Omega \times \lambda)\ &=\ \frac{1}{\zeta}\Omega, \\ (\Omega \times \lambda) \times \Omega - \nabla_\lambda \tilde{V}(\lambda)\ &=\ 0. \end{aligned} \tag{3.13}$$

It is easy to check that (3.13) are the first-order conditions for the variational principle,

$$\textit{make stationary}\ \ U(\Omega,\ \lambda) \qquad \textit{subject to}\ \ \frac{1}{2}\,|\Omega|^2\ =\ c, \tag{3.14}$$

where

$$U\ =\ \frac{1}{2}\ <\Omega,\ \mathbf{I}\Omega>\ +\ \frac{1}{2}\,|\Omega \times \lambda|^2\ -\ \tilde{V}(\lambda). \tag{3.15}$$

It is this variational principle that provides the starting point of our proof of the existence of relative equilibria. By further rearrangement, (3.13) can be rewritten as

$$(\mathbf{I} + \hat{\lambda}^T\hat{\lambda})\Omega = \beta\,\Omega, \tag{3.16a}$$

$$\hat{\Omega}^T\hat{\Omega}\lambda = \int_{\mathcal{B}} \frac{\lambda + Q}{|\lambda + Q|^3}\, d\nu(Q), \tag{3.16b}$$

$$\frac{1}{2}|\Omega|^2 = c. \tag{3.16c}$$

where $\hat{\lambda}^T\hat{\lambda}$ and $\hat{\Omega}^T\hat{\Omega}$ are 3×3 matrices constructed from the vectors λ and Ω through formula (2.2). By construction, solutions of (3.1) and solutions of (3.16) are in one-to-one correspondence.

It should be remarked that the Hamiltonian system (3.2) is the Poisson reduced system of (2.20) in the sense of Poisson reduction [13]. Relative equilibria characterized by (3.1) or (3.16) exactly coincide with the notion of relative equilibrium associated with the Poisson reduction. Accordingly, the principle of symmetric criticality [19] [28] can be applied, namely, the configuration components of the relative equilibria are the critical points of the *augmented potential* function, which for our problem is $-U$. Consequently, the variational principle (3.14) is a particular manifestation of the principle of symmetric criticality.

4. Great-circle Relative Equilibria

If we make the further assumption that the rigid body $\mathcal{B}$ has spherical symmetry, then it can be checked that the dynamical behavior of the center of mass C is exactly that of the Keplerian point mass model. It is well known that for a point mass moving in a central force field, the motion is constrained to a plane passing through the origin O. However, for an arbitrary rigid body, this may not be the case. In particular, at relative equilibrium, the radius vector from the origin O to the center of mass C may either trace a disc, or trace a cone, cf. Figure 4.1(a), (b). Those relative equilibria in which C traces a circle that resides on a plane passing the origin O will be termed *great-circle relative equilibria*. Otherwise, they will be called *non-great-circle relative equilibria*. In this section, we study only the great-circle relative equilibria.

From Figure 4.1(a), it is clear that the necessary and sufficient condition for great-circle relative equilibria is

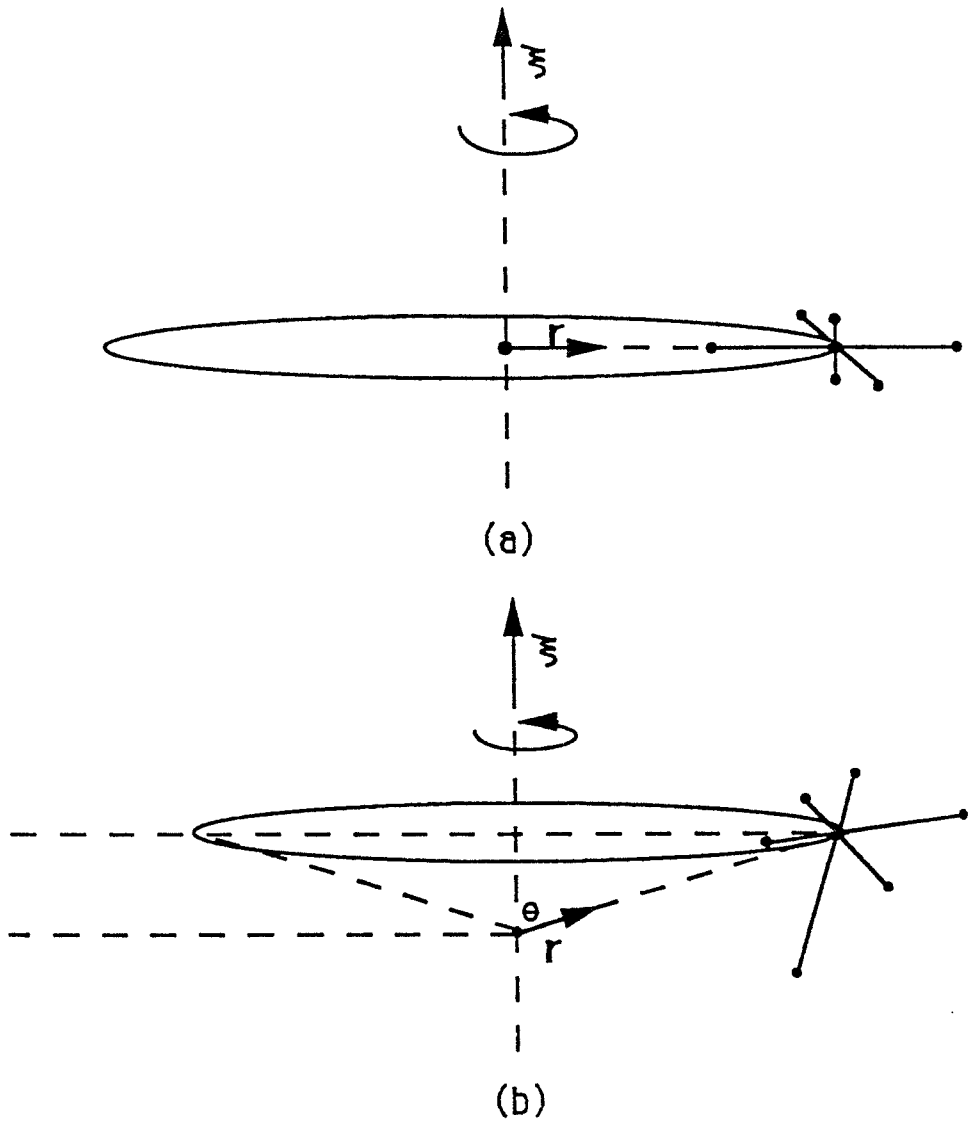

Figure 4.1. *(a)* Great-circle *vs.* *(b)* Non-great-circle *Relative Equilibria. Here* $r = B\lambda$ *is the radius vector in inertial frame, and* $\xi = B\Omega$ *points along the axis of rotation. The classic approximate analysis predicts great-circle orbits in which the orbit vector* r *sweeps out a disk. However, the Hamiltonian approach to the exact problem for asymmetric bodies predicts non-great-circle solutions in which* r *sweeps out a cone.*

$$\lambda \cdot \Omega \;=\; 0, \tag{4.1}$$

namely, the axis of rotation is perpendicular to the radius vector of C. Notice that equation (3.16a) can be rewritten as

$$\left(\mathbf{I} \;+\; |\lambda|^2 1 \;-\; \lambda\lambda^T\right)\Omega \;=\; \beta\,\Omega, \tag{4.2}$$

where $\mathbf{1}$ denotes the (3×3) identity matrix and $\lambda\lambda^T$ is a (3×3) rank one matrix. Thus for a great-circle relative equilibrium, in which $\lambda \cdot \Omega = 0$, we must have

$$\mathbf{I}\Omega \;=\; (\beta \;-\; |\lambda|^2)\,\Omega, \tag{4.3}$$

or equivalently Ω must be an eigenvector of the moment of inertia tensor. Moreover, condition (3.16b) reduces to

$$|\Omega|^2\lambda \;=\; \int_{\mathcal{B}} \frac{(\lambda \;+\; Q)}{|\lambda \;+\; Q|^3}\, dm(Q). \tag{4.4}$$

By regarding $|\Omega|^2$ in (4.4) as a Lagrange multiplier, it can be shown that (4.4) is the first-order condition for the variational problem,

$$\textit{make stationary} \qquad \tilde{V}(\lambda) \qquad \textit{subject to} \qquad \frac{1}{2}\,|\lambda|^2 \;=\; \tilde{c}, \tag{4.5}$$

where $\tilde{V}$ is defined in (3.10). In summary, in order for (Ω, λ, μ) to be a great-circle relative equilibrium, the vector λ must be a solution of the problem (4.5), and Ω must be an eigenvector of the inertia tensor, i.e. a principal axis. With condition (4.1), we then see that λ must also lie in a principal plane (i.e. a plane perpendicular to a principal axis).

The argument can be reversed. If there is a vector λ_0 solving the variational problem (4.5), there exists a multiplier κ such that

$$\nabla_\lambda \tilde{V}(\lambda_0) \;=\; \kappa\,\lambda_0. \tag{4.6}$$

Moreover, for physically relevant situations the rigid body does not overlap the center of the field. Thus

$$|\lambda|^2 \;+\; \lambda \cdot Q \;\geq\; |\lambda|^2 \;-\; |\lambda|\,|Q| \;=\; |\lambda|(|\lambda| - |Q|) \;>\; 0. \tag{4.7}$$

It can then be proved from (4.6) and (4.7) that the multiplier κ is necessarily positive. By comparing (4.6) and (3.16b) and if λ lies in a principal plane, we can construct a great-circle solution by picking $|\Omega|^2 = \kappa$, and Ω the principal axis with $\Omega \cdot \lambda = 0$. In fact, there are at least two such solutions corresponding to the choices Ω and $-\Omega$. Accordingly, if (4.6) holds for a λ_0 in a principal plane, we can find at least two great-circle relative equilibria. Furthermore, any plane of symmetry of the body $\mathcal{B}$ is necessarily a principal

plane, and there are at least two critical points of $\tilde{V}(\lambda)$ in the symmetry plane (a maximum and a minimum). As a consequence, we have the following theorem.

THEOREM 4.1.

For a rigid body having a plane of symmetry, there are at least four great-circle relative equilibria. Furthermore, if the rigid body is symmetric with respect to two planes, there are at least eight great-circle relative equilibria, and for a rigid body with three planes of symmetry, there are at least 24 great-circle relative equilibria.

∎

The second and third statements in Theorem 4.1 follow from similar arguments as those described above. The classic second-order approximate models analyzed in [11] implicitly assume that the body has three planes of symmetry, and they find exactly 24 great-circle relative equilibria.

5. Non-great-circle Relative Equilibria

In this section, we shall establish the existence of non-great-circle relative equilibria for non-symmetric bodies. We observed in the previous section that at a great-circle relative equilibrium, the variational problem (4.5) must have a solution λ lying in a principal plane. This fact can be used to prove that for some particular $\tilde{V}$ (i.e. for some particular rigid body $\mathcal{B}$), there are no great-circle relative equilibria, cf. [29], [27]. In particular, let the rigid body be a "molecule" consisting of six point masses, two on each principal axis, cf. Figure 5.1. (The molecule with unequal principal moments of inertia is an example in Beletskii [2] satisfying the conditions for the existence of relative equilibrium.) It was shown in [27] that if $x_1 \neq x_2$, $y_1 \neq y_2$, and $z_1 \neq z_2$, there is no great-circle relative equilibrium. Now if we could prove the existence of solutions to the problem (3.14), then for the cases in which there is no great-circle relative equilibrium, there must be a non-great-circle relative equilibrium. In fact, we shall show that for a general body, variational principle (3.14) is not useful for proving existence of relative equilibria. The difficulty is associated with "critical points at infinity", namely solutions in which Ω and λ are parallel with $|\lambda| \to \infty$. Fortunately, this difficulty can be finessed due to the pure

quadratic dependence upon Ω. We introduce another variational principle, namely

$$\begin{aligned} \textit{make stationary} \quad & \tilde{U}(\Omega,\ \lambda) \ = \ \frac{1}{2} < \Omega,\ \mathbf{I}\Omega > \ + \frac{1}{2} |\Omega \times \lambda|^2, \\ \textit{subject to} \quad & \frac{1}{2} |\Omega|^2 \ = \ c_1, \quad \text{and} \quad \tilde{V}(\lambda) \ = \ c_2, \end{aligned} \tag{5.1}$$

where we have introduced an additional artificial constraint with c_2 lying in the interval $(-\int_B (1/|Q|) d\nu(Q),\ 0)$. The Lagrangian associated with (5.1) is

$$L_{\tilde{U}} \ = \ \frac{1}{2} < \Omega,\ \mathbf{I}\Omega > \ + \frac{1}{2} |\Omega \times \lambda|^2 \ - \ \beta_1 (\frac{1}{2} |\Omega|^2 - c_1) \ - \ \beta_2 (\tilde{V}(\lambda) - c_2). \tag{5.2}$$

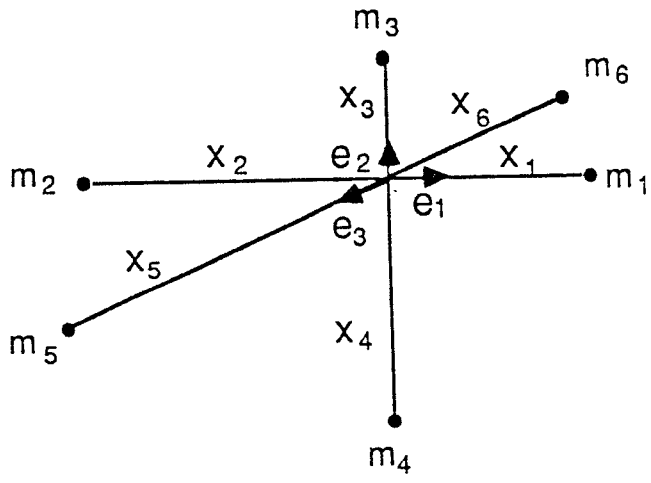

Figure 5.1. Molecule

Solutions of (5.1) with $\beta_2 = 1$ correspond to solutions of (3.14) for some value of c and therefore to relative equilibria. The first-order conditions associated with (5.2) are

$$(\mathbf{I} \ + \ \hat{\lambda}^T \hat{\lambda}) \Omega \ = \beta_1 \ \Omega, \tag{5.3a}$$

$$\hat{\Omega}^T \hat{\Omega} \lambda \ - \ \beta_2 \nabla_\lambda \tilde{V}(\lambda) \ = 0, \tag{5.3b}$$

$$\frac{1}{2} |\Omega|^2 \ = c_1, \tag{5.3c}$$

$$\tilde{V}(\lambda) \ = c_2. \tag{5.3d}$$

By taking the scalar product of λ with (5.3b), we get

$$\beta_2 \int_{\mathcal{B}} \frac{(|\lambda|^2 + \lambda \cdot Q)}{|\lambda + Q|^3}\, dm(Q) = \left(|\Omega|^2|\lambda|^2 - (\Omega \cdot \lambda)^2\right). \tag{5.4}$$

Notice that the right hand side of (5.4) is always nonnegative. On the other hand, from (4.7), it is seen that the multiplier β_2 of solutions of problem (5.1) must be nonnegative,

$$\beta_2 \geq 0, \tag{5.5}$$

with the equality holding if and only if Ω and λ are parallel.

We now compare conditions (5.3) and (3.16). It is clear that if there is a solution $(\tilde{\Omega},\ \tilde{\lambda},\ \tilde{\beta}_1,\ \tilde{\beta}_2)$ of (5.3) with $\tilde{\beta}_2 = 1$, then (3.16) is solved by $(\tilde{\Omega},\ \tilde{\lambda},\ \tilde{\beta}_1)$ with $c = c_1$. Moreover, since (5.3a) is linear in Ω, we can scale $\tilde{\Omega}$ arbitrarily without violating (5.3a). Accordingly, if we have a solution of (5.3) such that $\tilde{\beta}_2 > 0$, we obtain a solution $(\tilde{\Omega}/\sqrt{\tilde{\beta}_2},\ \tilde{\lambda},\ \tilde{\beta}_1)$ of (3.16) with $c = c_1/\tilde{\beta}_2$. On the other hand, the zeroth-order approximation of (5.3b) implies that $\tilde{\beta}_2 \simeq 2c_1/c_2^3$ (Kepler's frequency formula). Thus by holding c_1 fixed, and by varying c_2, we can achieve arbitrary $\tilde{\beta}_2$. The constant c is then also seen to be arbitrary. As a consequence, in order to prove the existence of solutions for problem (3.14) for some c, it suffices to find a solution of the problem (5.1) with $\tilde{\beta}_2 > 0$.

Next, we consider those extremals at which $\tilde{\beta}_2 = 0$. From (5.5), we see that for such extremals $\tilde{\Omega}$ is parallel to $\tilde{\lambda}$, which, in turn, shows that $\tilde{\Omega}$ must be an eigenvector of $\mathbf{I}$, say

$$\mathbf{I}\tilde{\Omega} = I_1\tilde{\Omega},$$

or $\tilde{\beta}_1 = I_1$, cf. (5.3a). It is then easy to check that the objective function $\tilde{U}(\Omega, \lambda)$ cannot assume its minimum value at such extremal points. In fact, the Hessian of $L_{\tilde{U}}$ for $\beta_2 = 0$ can be found to be

$$D^2_{(\Omega,\lambda)} L_{\tilde{U}} = \begin{pmatrix} \mathbf{I} + \hat{\lambda}^T\hat{\lambda} - I_1\mathbf{1} & 2\hat{\lambda}\hat{\Omega} - \hat{\Omega}\hat{\lambda} \\ 2\hat{\Omega}\hat{\lambda} - \hat{\lambda}\hat{\Omega} & \hat{\Omega}^T\hat{\Omega} \end{pmatrix}, \tag{5.6}$$

and the tangent space at $(\tilde{\Omega}, \tilde{\lambda})$ to the constrained subspace can be expressed as,

$$\mathcal{D} = \{\ (y_1, y_2) \in \mathbb{R}^6 \ :\ \tilde{\Omega} \cdot y_1 = 0,\ \nabla_\lambda \tilde{V}(\tilde{\lambda}) \cdot y_2 = 0\ \}.$$

Since $\tilde{\Omega}$ is a principal axis of the rigid body $\mathcal{B}$, the vector y_1 must be in a principal plane. We compute

$$\begin{aligned}
&(y_1^T\ 0)\ D^2_{(\Omega,\lambda)} L_{\tilde{U}}(\tilde{\Omega},\tilde{\lambda})\ \begin{pmatrix} y_1 \\ 0 \end{pmatrix} \\
&\quad = y_1^T \mathbf{I} y_1 \ + (\tilde{\lambda} \times y_1)^2 \ - \ I_1 |y_1|^2 \\
&\quad \geq \left(|\tilde{\lambda}|^2 \ - \ (I_1 - \min\{I_i\}) \right) |y_1|^2,
\end{aligned}$$

since we also have $\tilde{\lambda} \cdot y_1 = 0$. Moreover, through the non-dimensionalization process, we have $tr(\mathbf{I}) = 1$, which implies $|I_1 - \min\{I_i\}| < 1$. Thus with the natural assumption $|\lambda| > 1$, cf. (4.7), the difference $|\tilde{\lambda}|^2 \ - \ (I_1 - \min\{I_i\})$ is always positive. Consequently, the quadratic form of the Hessian restricted to $\mathcal{D}$ can never be negative-semidefinite. This implies that the critical point with $\tilde{\beta}_2 = 0$ can never be a maximizer for the problem (5.1). However, problem (5.1) has a continuous objective function $\tilde{U}$ on a closed and bounded constraint set. It follows that there must be a maximizer for the problem. The above argument reveals that this maximizer must be a critical point with $\tilde{\beta}_2 > 0$. As a consequence, there must be a solution for the problem (5.4). Recall that for the molecule example, cf. Figure 5.1, there is no great-circle relative equilibrium. Thus the solution whose existence is proven here must give rise to a non-great-circle relative equilibrium.

More detailed information can be obtained by applying Morse theory to this problem. The variational principle (5.1) can be re-stated as finding critical points of $\tilde{U}$ on the manifold $\mathbb{RP}^2 \times S^2$, by modding out the $\mathbb{Z}_2$ symmetry on Ω. It can be checked that the Betti numbers for the manifold $\mathbb{RP}^2 \times S^2$ are $\beta_0 = 1$, $\beta_1 = 1$, $\beta_2 = 2$, $\beta_3 = 1$, $\beta_4 = 1$. On the other hand, the indices of the critical points with $\beta_2 = 0$ can be found by counting the number of negative eigenvalues of the Hessian (5.6) restricted to the tangent space $\mathcal{D}$. It turns out that there are two solutions for each index 0, 1, and 2. Now invoking the Morse inequalities [16], we conclude there is at least one solution for each of the indices 3 and 4, respectively. Consequently, by including the $\mathbb{Z}_2$ symmetry, it may be concluded that there are at least four non-great-circle relative equilibria.

In [1], a proof for the existence of non-great-circle relative equilibria for approximate models was given based on the assumptions that the principal central moments of inertia

are not equal, and the body size is sufficiently small in comparison with the distance to the center of the field. The variational proof given above applies to the exact model as well as to its approximations and makes less restrictive hypotheses.

6. A Numerical Search and Error Analysis

The existence of non-great-circle relative equilibria for certain bodies $\mathcal{B}$ are ensured by the arguments presented in the previous section. We now seek such relative equilibria numerically, and justify the statement that while the offset of the circular orbit is necessarily very small, the associated attitude change may be quite significant. The numerical method adopted and the associated error analysis are described in this Section. Specific examples will be given in Section 7.

We consider the example of a molecule as depicted in Figure 5.1. Recall that the conditions for relative equilibria are given in (3.16), which can be rewritten as

$$|\Omega|^2\lambda \;-\; (\Omega\cdot\lambda)\Omega \;-\; A\sum_{i=1}^{6}\frac{m_i(\lambda+Q_i)}{|\lambda+Q_i|^3} \;=\; 0, \tag{6.1a}$$

$$\mathbf{I}\Omega \;+\; |\lambda|^2\Omega \;-\; (\Omega\cdot\lambda)\lambda \;+\; \beta\,\Omega \;=\; 0, \tag{6.1b}$$

$$\frac{1}{2}\,|\Omega|^2 \;-\; c \;=\; 0, \tag{6.1c}$$

where

$$Q_1 \;=\; \begin{pmatrix} x_1 \\ 0 \\ 0 \end{pmatrix},\; Q_2 \;=\; \begin{pmatrix} -x_2 \\ 0 \\ 0 \end{pmatrix},\; Q_3 \;=\; \begin{pmatrix} 0 \\ x_3 \\ 0 \end{pmatrix},$$

$$Q_4 \;=\; \begin{pmatrix} 0 \\ -x_4 \\ 0 \end{pmatrix},\; Q_5 \;=\; \begin{pmatrix} 0 \\ 0 \\ x_5 \end{pmatrix},\; Q_6 \;=\; \begin{pmatrix} 0 \\ 0 \\ -x_6 \end{pmatrix},$$

and A is a parameter included for numerical purposes. Physically the parameter A is associated with scaling in time. It will be chosen later to minimize numerical ill-conditioning. Equation (6.1) comprise a nonlinear system of seven equations in seven unknowns $(\lambda, \Omega, \beta) \in \mathbb{R}^7$. A numerical continuation method will be used to find solutions of these equations, and therefore to yield relative equilibria.

First we make some observations. It has been proven that if a molecule is asymmetric, there is no great-circle relative equilibrium. Thus for the purpose of illustrating examples of non-great-circle relative equilibria it suffices to consider bodies of this very special type. On the other hand, if the molecule is symmetric (i.e. $x_1 = x_2$, $x_3 = x_4$, $x_5 = x_6$), there are 24 great-circle relative equilibria which are known explicitly. Such explicit solutions will be the starting points for our continuation methods. Consider the following case

$$\lambda = \begin{pmatrix} a \\ 0 \\ 0 \end{pmatrix}, \qquad \Omega = \begin{pmatrix} 0 \\ b \\ 0 \end{pmatrix}. \tag{6.2}$$

We have

$$A\sum_{i=1}^{6} \frac{m_i(\lambda + Q_i)}{|\lambda + Q_i|^3} = A \begin{pmatrix} \frac{m_1}{(a+x_1)^2} + \frac{m_2}{(a-x_2)^2} + \sum_{i=3}^{6} \frac{m_i a}{\sqrt{a^2+x_i^2}^3} \\ \frac{m_3 x_3}{\sqrt{a^2+x_3^2}^3} - \frac{m_4 x_4}{\sqrt{a^2+x_4^2}^3} \\ \frac{m_5 x_5}{\sqrt{a^2+x_5^2}^3} - \frac{m_6 x_6}{\sqrt{a^2+x_6^2}^3} \end{pmatrix}$$

$$= A \begin{pmatrix} \frac{m_1}{(a+x_1)^2} + \frac{m_2}{(a-x_2)^2} + \frac{2m_3 a}{\sqrt{a^2+x_3^2}^3} + \frac{2m_5 a}{\sqrt{a^2+x_5^2}^3} \\ 0 \\ 0 \end{pmatrix},$$

because of the symmetry of the molecule. Thus (6.1a) can be reduced to

$$ab^2 - A\left(\frac{m_1}{(a+x_1)^2} + \frac{m_2}{(a-x_2)^2} + \frac{2m_3 a}{\sqrt{a^2+x_3^2}^3} + \frac{2m_5 a}{\sqrt{a^2+x_5^2}^3}\right) = 0, \tag{6.3}$$

Similarly for solutions of the form (6.2), equation (6.1b) reduces to

$$I_2 b + a^2 b - \beta b = 0.$$

With a, $b = \sqrt{2c}$, and β satisfying (6.3) and

$$\beta = -(I_2 + a^2), \tag{6.4}$$

then λ, Ω of the form (6.2) provide a solution of (6.1), and are thus a relative equilibrium. Similar arguments can be applied to all other great-circle solutions. With the solutions for symmetric cases as starting points, it is possible to follow the path of solutions by numerical continuation as the parameters are varied to the desired asymmetric case.

The numerical continuation or path-following method is discussed in many places, see e.g. [10] [30] [8], and references therein. The basic idea is to solve a sequence of

problems as a parameter is varied, starting with a known solution, so that at each step a locally convergent algorithm can be applied to yield the new solution, which will form the starting point for the next iteration. A homotopy provides the linkage between the known simple solutions, and the desired answer. Since in our problem the relative equilibria for a symmetric molecule are simply obtained by solving (6.3), it is natural to start the homotopy from these symmetric cases. Let (6.1) be represented as

$$F(m_1, m_2, m_3, m_4, m_5, m_6, \lambda, \Omega, \beta) \;=\; 0. \tag{6.5}$$

For a completely asymmetric molecule, we have $m_1 \neq m_2$, $m_3 \neq m_4$, and $m_5 \neq m_6$. Define

$$m_x \;=\; \frac{m_1 + m_2}{2}, \quad m_y \;=\; \frac{m_3 + m_4}{2}, \quad m_z \;=\; \frac{m_5 + m_6}{2}.$$

Three homotopies will be used in series to fulfill the path-following process, namely,

$$H_1(\lambda, \Omega, \beta, \tau) = F(\tau m_1 + (1-\tau)m_x, \tau m_2 + (1-\tau)m_x, m_y, m_y, m_z, m_z, \lambda, \Omega, \beta), \tag{6.6a}$$

$$H_2(\lambda, \Omega, \beta, \tau) = F(m_1, m_2, \tau m_3 + (1-\tau)m_y, \tau m_4 + (1-\tau)m_y, m_z, m_z, \lambda, \Omega, \beta), \tag{6.6b}$$

$$H_3(\lambda, \Omega, \beta, \tau) = F(m_1, m_2, m_3, m_4, \tau m_5 + (1-\tau)m_z, \tau m_6 + (1-\tau)m_z, \lambda, \Omega, \beta). \tag{6.6c}$$

By slowly varying τ at each stage, locally convergent algorithms such as the Newton-Raphson method lead to the desired solutions. In order to successfully find the solutions of (6.3), we note the fact that for $\lambda \cdot \Omega = 0$ and $|\lambda| \gg \max\{x_i, i = 1, \cdots, 6\}$,

$$|\lambda|^3 |\Omega|^2 \;\simeq\; A, \tag{6.7}$$

which is the Kepler's frequency formula for the zeroth order approximate model, cf. [29]. Accordingly, for given A, (6.3) can be solved by choosing the initial value $(A/b^2)^{1/3}$.

The above path-following method will later be termed *method of continuation in mass*. We now study the local numerical algorithm for finding solutions at each step along the path. Due to the smallness of the ratio between the body size (the x_i) and the radius $|\lambda|$, the numerical search for solutions of (6.1) becomes highly ill-conditioned. The constant A plays an important role in making our numerical methods tractable. Before performing

the error analysis, we describe a theorem of Kantorovich which will play a pivotal role in proving that actual solutions lie close to our numerical approximates.

THEOREM 6.1. (Kantorovich)

Let $D \subset \mathbb{R}^n$ be an open set, $F : D \to \mathbb{R}^n$ be continuously differentiable, and the matrix F' be Lipschitz continuous in D with Lipschitz constant α. Let $x_0 \in D$, with $F'(x_0)$ nonsingular, and suppose there are positive constants σ and γ such that $\|F'(x_0)^{-1}\| \leq \sigma$, $\|F'(x_0)^{-1} F(x_0)\| \leq \gamma$, and $h \triangleq \alpha\sigma\gamma < 1/2$. Set $e^* = (1-\sqrt{1-2h})/\alpha\sigma$. Let $B(x_0, e^*)$ be the open ball with center x_0 and radius e^*, and suppose further that h is so small that $B(x_0, e^*) \subset D$. Then there is a unique $x^* \in B(x_0, e^*)$ with $F(x^*) = 0$. ∎

The proof of this theorem can be found in [10], [18], or [17]. The first part of the theorem provides a way to measure the error bound for the approximate solutions, and could also serve as a criterion for convergence. In particular, if an approximate solution satisfies the conditions

$$\gamma < \epsilon, \qquad \alpha\sigma\gamma < 1/2, \tag{6.8}$$

then the error of this approximate solution is bounded by ϵ. As a consequence, condition (6.8) can be used to guarantee the convergence of an algorithm.

In order to apply Theorem 6.1 to our problem, a value of A (appearing in (6.1)) muct be chosen and there are some constants to be determined. The detailed derivation of these constants is presented in Appendix B. Here we summarize the results by noting that the conditions on A are given by, cf. (B.9), (B.15),

$$A \sim |\lambda|^4, \quad \text{and} \quad A < \frac{|\lambda|^5}{72 m_{\max}}, \tag{6.9}$$

and suitable forms for the constants appearing in Theorem 6.1 are, cf. (B.3), (B.12), and (B.17),

$$\gamma = \max\{\delta x_i,\ i = 1, \cdots, n\}, \quad \sigma = \frac{n}{\rho_{\min}}, \quad \text{and} \quad \alpha \simeq 2n|\lambda|. \tag{6.10}$$

Here δx solves (B.11), and $\rho_{\min}$ is the minimum eigenvalue of $F'(\lambda, \Omega, \beta)$. With those constants determined through (6.10), criteria (6.8) can be applied to the Newton-Raphson

method to find approximate solutions with an associated error bound. The constant A determined from (6.9) makes it possible to deal with numerical ill-conditioning. These considerations will be further described in the next section.

7. Examples

In this section, the ideas described in Section 6 are combined to generate an algorithm which finds non-great-circle relative equilibria. Here, we only look at simple models, namely a rigid body $\mathcal{B}$ with the structure of a molecule, but in principle, the methods we use could be extended to more complicated mass distributions. In the first example, the parameters of the molecule are motivated by the parameters of the motion of the satellite Phobos around the planet Mars. Non-great-circle relative equilibria with small deviations from the classic solutions are are numerically found. We then fix the size of the molecule and the radius of the orbit $|\lambda|$, and study the effects of different moments of inertia on the relative equilibria. The second example is artificial, but does include the parameter regimes in which a space station orbiting the Earth would fall, and serves as a demonstration of large orientation change from the classical solutions. Here, while holding the mass distribution and the moments of inertia of the molecule fixed, a branch of non-great-circle relative equilibria starting with $|\lambda| = 500$ and ending with $|\lambda| = 40000$ is obtained. In all examples, the Newton-Raphson method is used to find solutions in each step of the continuation method. With the error criteria (6.8), we revise the standard algorithm as follows.

ALGORITHM 7.1.

1. Give x_0. Set $k = 0$. Specify ϵ.
2. Find δx such that
$$F'(x_k)\,\delta x \;=\; F(x_k).$$
3. Let $\gamma = \max\{\delta x_i,\ i = 1,7\}$. Evaluate α, σ. If $\gamma < \epsilon$ and $\alpha\sigma\gamma < 1/2$, EXIT.
4. $x_{k+1} = x_k + \delta x$. $k = k + 1$. Goto 2.

∎

In Step 2, the singular value decomposition of $F'(x_k)$ is found first. This not only takes care of the problem of ill-conditioning, but also provides us with the smallest singular value which leads to the constant σ, cf. (6.10). The other constant α can also be obtained from (6.10). As guaranteed by Theorem 6.1, if Algorithm 7.1 successfully converges to an $\bar{x}$, there must exist a solution x^* nearby. The error bound is given by ϵ, which will be chosen to be 10^{-8}. In the following examples, every solution is obtained through this Algorithm, and is thus a bona-fide approximate solution.

7.1. Phobos

We consider the case of the satellite Phobos moving around the planet Mars. The related data for our study is included in Appendix A, cf. [15]. In the process of nondimensionalization, the scales are chosen to be, cf. (2.14),

$$mass: \ m = 1.082 \times 10^{16} \ (kg), \qquad length: \ l \ = \ \sqrt{\frac{tr(\mathbf{I}^*)}{m}} \ = \ 12.4 \ (km). \tag{7.1}$$

The time scale is irrelevant here, since we are interested in relative equilibria. Accordingly, the scaled radius is about $|\lambda| = 760$. Also the non-dimensional moments of inertia are

$$\mathbf{I} \ = \ \begin{pmatrix} 0.3294 & 0 & 0 \\ 0 & 0.2825 & 0 \\ 0 & 0 & 0.3881 \end{pmatrix}. \tag{7.2}$$

Now we assume that Phobos is in the shape of an ellipsoid with the above inertia and uniform mass distribution. The axes of the ellipsoid can be found through elementary analysis to be 1.847, 2.086, 1.496. We next look for the most asymmetric molecule fitting inside the ellipsoid (cf. Figure 7.1) to get the most interesting non-great-circle relative equilibria. Physically this procedure might be interpreted as seeking the largest possible orbit deviation due to non-uniform mass distribution consistent with an observed shape. The center of molecule is set to coincide with the center of the ellipsoid. The constants α, σ for this example are approximately 10^4, and 10^3 respectively. It was found that with

$$x_1 \ = \ 0.9236, \quad x_2 \ = \ 0.4618, \quad x_3 \ = \ 1.043,$$

$$x_4 \ = \ 0.5214, \quad x_5 \ = \ 0.748, \quad x_6 \ = \ 0.748,$$

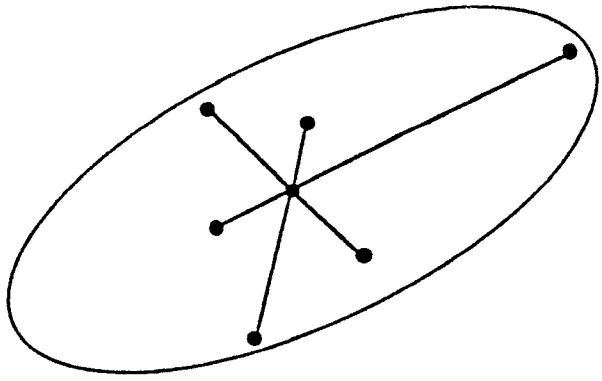

Figure 7.1. Molecule inside the ellipsoid of Phobos

we obtain the following non-great-circle relative equilibrium,

$$\lambda = (759.999, 1.215, -1.3 \times 10^{-10}),$$

$$\Omega = (2.6 \times 10^{-11}, 0.000, 152.0), \quad \beta = -577600.40.$$

In spherical coordinates (r, θ, ϕ), the vector $\lambda = (r\cos\phi\cos\theta,\ r\cos\phi\sin\theta,\ r\sin\phi)$ can be represented as $(760.00, 0.0916, 0.000)$. Here θ and ϕ are in degrees. Clearly this relative equilibrium is very close to the great-circle case in which λ is $(760, 0, 0)$. In order to construct interesting non-great-circle relative equilibria, we hold the size of the molecule and the third moment of inertia (0.3881) fixed, while varying the other two moments of inertia. We obtain a family of relative equilibria as listed in Table 7.2, where the norms of λ and Ω are 760 and 152, respectively. The notations $\theta(\lambda)$ and $\phi(\lambda)$ denote spherical coordinates of the vector λ (in degrees).

Figure 7.3 shows the configuration of the molecule at relative equilibrium for the case of $I_1 = 0.305956$, $I_2 = 0.305935$ in Table 7.2. The molecule rotates approximately 40.13 degrees about the vertical axis. Here we see the effects of nearly equal moments of inertia in changing the configurations at relative equilibria. It is observed in Table 7.2 that as the moments of inertia approach each other, the molecule at relative equilibrium exhibits significant change in orientation from the classical solutions.

We remark that, in [29], it was shown that there is no non-great-circle relative equilibrium for the second-order approximate model with large $|\lambda|$. Here the second-order approximate model refers to the model with the approximation of the potential function $\tilde{V}(\lambda)$ defined in (3.10) as

I_1	I_2	$\theta(\lambda)$	$\phi(\lambda)$	$\theta(\Omega)$	$\phi(\Omega)$
0.329386	0.282505	0.0916	0.0000	0.0509	90.000
0.325386	0.286505	0.1094	0.0000	0.0675	90.000
0.320086	0.291805	0.1485	0.0000	0.1049	90.000
0.315186	0.296705	0.2251	0.0000	0.1796	90.000
0.310036	0.301855	0.5087	0.0000	0.4604	90.000
0.308036	0.303855	1.0152	0.0000	0.9648	90.000
0.306886	0.305005	2.3956	0.0000	2.3414	90.000
0.306636	0.305255	3.3944	0.0000	3.3379	90.000
0.306436	0.305455	5.0607	0.0000	5.0010	90.000
0.306336	0.305555	6.6530	0.0000	6.5906	90.000
0.306236	0.305655	9.5089	0.0000	9.4431	90.000
0.306131	0.305760	15.7147	0.0000	15.6474	90.000
0.306086	0.305805	20.2084	0.0000	20.1450	90.000
0.306066	0.305825	22.6487	0.0000	22.5890	90.000
0.306016	0.305875	29.8738	0.0000	29.8313	90.000
0.305996	0.305895	33.1418	0.0000	33.1095	90.000
0.305956	0.305935	40.1303	0.0000	40.1231	90.000

Table 7.2. Relative Equilibria for Molecules of Different Inertias at Constant Orbit Radius $|\lambda|$

$$\tilde{V}(\lambda) \simeq -\frac{1}{|\lambda|} - \frac{1}{2|\lambda|^3} + \frac{3}{2|\lambda|^5} < \lambda, \mathbf{I}\lambda > .$$

In order to have this second-order model fail to be a valid approximation, we expect to have inertias close to each other. Of course, inertial spherical symmetry does not necessarily imply a spherically symmetric body, so that the body may be subjected to higher-order terms, cf. [14]. Our numerical investigation is in accord with the above observations.

In [1], small deviations from great-circle relative equilibria were found as perturbations of solutions to the approximate model. The numerical results presented here show that with two nearly equal moments of inertia, the exact problem may have non-great-circle relative equilibria with large changes in orientation from the solutions of the classic approximate model.

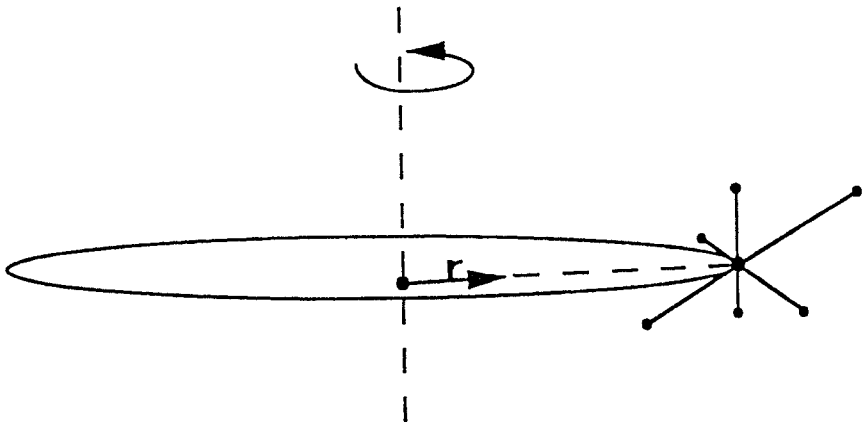

Figure 7.3. Configuration of a Non-great-circle Relative Equilibrium

7.2. Example with Branches of Solutions Parametrized by $|\lambda|$

We consider a molecule with the following data,

$$\begin{aligned} m_1 &= 0.330066, \quad m_2 = 0.00330033, \\ m_3 &= 0.330033, \quad m_4 = 0.00330033, \\ m_5 &= 0.33, \quad m_6 = 0.00330033, \\ I_1 &= 0.3332, \quad I_2 = 0.3335, \quad I_3 = 0.3333, \end{aligned} \tag{7.3}$$

moving in a central gravitational field. The intuitive idea behind devising example (7.3) is to choose the moments of inertia close to each other so as to emphasize the importance of higher-order terms, while the mass distribution is designed such that the body is structurely highly asymmetric. In particular, the ratios of masses are 101, 100, and 99 for each principal axis, respectively.

The method of continuation in mass discussed in Section 5 has been used with Algorithm 7.1 to find relative equilibria for selected $|\lambda|$ from 500 to 40,000. We remark here that the nondimensional parameter regime overlaps the range in which Earth orbiting artificial satellites may lie. For example, the space station Freedom has been designed to have maximum dimension 0.2 (km) and orbit with radius 6,800 (km). Thus the scaled $|\lambda|$ is approximately 34,000, which falls within the examined range. With some experimentation, it was observed that with the initial point,

$$\lambda = \begin{pmatrix} 0 \\ |\lambda| \\ 0 \end{pmatrix}, \qquad \Omega = \begin{pmatrix} |\Omega| \\ 0 \\ 0 \end{pmatrix}, \qquad \beta = -|\lambda|^2, \tag{7.4}$$

in the method of continuation in mass, the most interesting solutions were obtained. However, in finding solutions for large $|\lambda|$, for example $|\lambda| = 20,000$, the constants are approximately

$$\alpha \simeq 10^6, \qquad \sigma \simeq 10^5,$$

which implies that we need to have the constant $\gamma < 10^{-12}$ to fulfill the condition $\alpha\sigma\gamma < 0.5$. Because for these solutions $|\lambda| \sim 10^5$, the 16-digit accuracy available in double precision on a typical 32-bit machine (e.g. a Sun Workstation) is inadequate. We therefore ran our program on a CRAY supercomputer which provides 29 significant digits in double precision, cf. e.g. [20]. Table 7.4 lists those relative equilibria thereby obtained with λ, Ω represented in their spherical coordinates.

$\|\lambda\|$	$\theta(\lambda)$	$\phi(\lambda)$	$\|\Omega\|$	$\theta(\Omega)$	$\phi(\Omega)$
500	46.8611	-17.4627	100	-54.7456	-32.6009
760	47.8276	-17.8208	152	-54.7761	-34.1683
1000	48.7091	-18.1277	200	-54.8384	-35.5845
3000	55.3232	-17.2751	600	-20.2429	38.7129
6000	65.6627	-19.5986	1200	-15.6572	22.9702
8000	71.0045	-22.9513	1600	-11.4520	17.2236
9000	73.0742	-25.3278	1800	-9.5049	15.2639
12000	78.0382	22.8848	2400	-7.5808	-10.2578
15000	81.2009	18.9175	3000	-6.4284	-6.8820
20000	84.1137	13.7814	4000	-4.9693	-3.7331
30000	86.5362	8.1721	6000	-3.2604	-1.4159
40000	87.5514	5.6183	8000	-2.3792	-0.7051

Table 7.4. Relative Equilibria Illustrating Large Orientation Drifts

Interestingly, there are three segments of distinct branches of solutions shown in Table 7.4, namely, those with $|\lambda|$ in the range of 500–1,000, 3,000–9,000, and 12,000–40,000. We conjecture that there are some bifurcation or turning points in the (λ, Ω, β) space. In order to construct one branch completely, we abandoned continuation in the masses, and instead started with solutions at $|\lambda| = 12,000$ and reduced the radius $|\lambda|$ with numerical continuation until $|\lambda| = 500$. On the CRAY, this method of continuation in radius successfully gives us the branch of solutions listed in Table 7.5. It can be seen that the solution branch for $|\lambda| = 500$–1000 in Table 7.4 is disconnected from the branch starting from $|\lambda| = 12{,}000$–40,000 that is continued in Table 7.5 down to small radii.

$\lvert\lambda\rvert$	$\theta(\lambda)$	$\phi(\lambda)$	$\lvert\Omega\rvert$	$\theta(\Omega)$	$\phi(\Omega)$
500	46.7440	35.1556	100	-10.1838	-37.7702
1000	48.5200	35.0055	200	-10.3029	-36.4710
2000	52.0762	34.5767	400	-10.4690	-33.7789
3000	55.5958	33.9734	600	-10.5296	-30.9911
4000	59.0231	33.1958	800	-10.4787	-28.1563
5000	62.3003	32.2504	1000	-10.3185	-25.3351
6000	65.3718	31.1514	1200	-10.0596	-22.5938
7000	68.1912	29.9214	1400	-9.7205	-19.9952
8000	70.7275	28.5895	1600	-9.3239	-17.5892
9000	72.9684	27.1885	1800	-8.8934	-15.4074
10000	74.9195	25.7512	2000	-8.4496	-13.4624
11000	76.6003	24.3081	2200	-8.0085	-11.7507
12000	78.0382	22.8848	2400	-7.5808	-10.2578
15000	81.2009	18.9175	3000	-6.4284	-6.8820
20000	84.1137	13.7814	4000	-4.9693	-3.7331
25000	85.6324	10.3865	5000	-3.9630	-2.2060
30000	86.5362	8.1721	6000	-3.2604	-1.4159
34000	87.0289	6.9333	6800	-2.8441	-1.0438
35000	87.1310	6.6760	7000	-2.7551	-0.9729
40000	87.5514	5.6183	8000	-2.3792	-0.7051

Table 7.5. A Branch of Non-great-circle Relative Equilibria

It would be interesting to find the other branches completely. However, more delicate numerical tools need to be applied. In particular, a continuation code designed to traverse turning points is apparently required. This problem is currently under investigation.

8. Conclusions

In this paper, we have proven the existence of non-great-circle relative equilibria for the exact model of motion of a rigid body in a central gravitational field. A coordinate-free approach was adopted to avoid singularities and cumbersome manipulations inherent to local coordinates, such as Euler angles. Numerical methods for finding the relative equilibria with an associated delicate error analysis have been presented. The numerical solutions we obtained demonstrate that the non-great-circle relative equilibria may exhibit large orientation changes from the classic approximate solutions for bodies with nearly equal moments of inertia. If these relative equilibria prove to be stable, the attitude design of spacecraft might be able to take advantage of such configurations to yield effective attitude control strategies.

ACKNOWLEDGEMENT.

We are happy to thank J. Alexander, A. Bahri, H. Brezis, B. Kellogg, and J. Miller for helpful discussions.

Appendix A. Data for Phobos around Mars

Phobos mass $\simeq \quad 1.082 \times 10^{16}\ (kg)$.

Phobos volume $\simeq \quad 5.673 \times 10^{3}\ (km^3)$.

Phobos principal moments of inertia

$$\mathbf{I}^* \simeq \begin{pmatrix} 5.50 & 0 & 0 \\ 0 & 4.718 & 0 \\ 0 & 0 & 6.481 \end{pmatrix} \times 10^{17}\ (kg \cdot km^2).$$

Phobos orbit radius (major semi-axis) $\simeq \quad 9,378.5\ (km)$.

Phobos radius $\simeq \quad 11.1\ (km)$.

Mars radius $\simeq$ $3,394\ (km)$.

Appendix B. Determining Constants in Theorem 5.1.

In this Appendix, we discuss the issue of determining the constants in Theorem 6.1 as well as how to pick a suitable constant A to make the problem numerically tractable. We first look at σ, the constant associated with the Jacobian of F. Since (6.1) comes from a variational principle, the derivative of F in (6.5) with respect to λ, Ω, and β is a 7×7 symmetric matrix with real eigenvalues. Let $\rho_{\min}$ denote the minimum eigenvalue of $F'(\lambda, \Omega, \beta)$. It is easy to see that $1/\rho_{\min}$ is the maximum eigenvalue of $F'(\lambda, \Omega, \beta)^{-1}$. Thus

$$\|F'(\lambda, \Omega, \beta)^{-1}\|_2 \ \leq \ \frac{1}{\rho_{\min}}, \tag{B.1}$$

where $\|\cdot\|_2$ denotes the matrix or operator norm induced from the usual vector 2-norm on $\mathbb{R}^n$. Accordingly, if the 2-norm is used, σ could be specified as $1/\rho_{\min}$. On the other hand, if the sup-norm defined by $\|x\|_\infty = \max\{|x_i|, i = 1, n\}$ is selected, because of the inequalities

$$\|x\|_\infty \ \leq \ \|x\|_2 \ \leq \ n\|x\|_\infty, \qquad \text{for } x \in \mathbb{R}^n,$$

we have

$$\|F'(\lambda, \Omega, \beta)^{-1}\|_\infty \ \leq \ n\|F'(\lambda, \Omega, \beta)^{-1}\|_2 \ \leq \ \frac{n}{\rho_{\min}}. \tag{B.2}$$

The constant σ can then be chosen as

$$\sigma \ = \ \frac{n}{\rho_{\min}}. \tag{B.3}$$

Since it is considerably more convenient to use the sup-norm in determining the Lipschitz constant for F', the σ defined in (B.3) will be adopted.

In order that conditions (6.8) can hold, it is evident that σ cannot be too large, or equivalently, $\rho_{\min}$ cannot be too small. In order to have a measure of $\rho_{\min}$, we consider the special case of the relative equilibrium (6.2) for a symmetric molecule.

The Jacobian of F can be found from (6.1) to be the symmetric matrix,

$$F'(\lambda,\Omega,\beta) = \begin{pmatrix} (|\Omega|^2 - \sum_{i=1}^6 \frac{Am_i}{|\lambda+Q_i|^3}\mathbf{1} - \Omega\Omega^T \\ +\sum_{i=1}^6 \frac{3Am_i}{|\lambda+Q_i|^5}(\lambda+Q_i)(\lambda+Q_i)^T & -(\lambda\cdot\Omega)\mathbf{1} + 2\lambda\Omega^T - \Omega\lambda^T & 0 \\ \cdots & \mathbf{I} + (|\lambda|^2+\beta)\mathbf{1} - \lambda\lambda^T & \Omega \\ \cdots & \cdots & 0 \end{pmatrix}. \tag{B.4}$$

Evaluation of F' at the particular relative equilibrium (6.2) and (6.4) yields the following simplified matrix,

$$J = \begin{pmatrix} J_{11} & 0 & 0 & 0 & 2ab & 0 & 0 \\ 0 & J_{22} & 0 & -ab & 0 & 0 & 0 \\ 0 & 0 & J_{33} & 0 & 0 & 0 & 0 \\ 0 & -ab & 0 & I_1 - I_2 - a^2 & 0 & 0 & 0 \\ 2ab & 0 & 0 & 0 & 0 & 0 & b \\ 0 & 0 & 0 & 0 & 0 & I_3 - I_2 & 0 \\ 0 & 0 & 0 & 0 & b & 0 & 0 \end{pmatrix}, \tag{B.5}$$

where

$$J_{11} = b^2 + A\left(\frac{3m_1}{(a+x_1)^3} + \frac{3m_1}{(a-x_1)^3} + \frac{6m_3a^2}{\sqrt{a^2+x_3^2}^5} + \frac{6m_5a^2}{\sqrt{a^2+x_5^2}^5} - \sum_{i=1}^6 \frac{m_i}{|\lambda+Q_i|^3}\right), \tag{B.6a}$$

$$J_{22} = A\left(\frac{6m_3x_3^2}{\sqrt{a^2+x_3^2}^5} - \sum_{i=1}^6 \frac{m_i}{|\lambda+Q_i|^3}\right), \tag{B.6b}$$

$$J_{33} = b^2 + A\left(\frac{6m_5x_5^2}{\sqrt{a^2+x_5^2}^5} - \sum_{i=1}^6 \frac{m_i}{|\lambda+Q_i|^3}\right). \tag{B.6c}$$

The characteristic polynomial of J is

$$\begin{aligned} \det(s\mathbf{1} - J) = {} & (s - J_{33})(s - (I_3 - I_2)) \\ & \left(s^2 - (J_{22} + I_1 - I_2 - a^2)s + J_{22}(I_1 - I_2 - a^2) - a^2b^2\right) \\ & \left(s^3 - J_{11}s^2 - (1+4a^2)b^2s + J_{11}b^2\right). \end{aligned} \tag{B.7}$$

There are two obvious eigenvalues of J, namely, J_{33} and $I_3 - I_2$. The second is given by body parameters, and, in our nondimensionalization, has absolute value smaller than one. With (6.7), J_{33} in (B.6c) can be approximated as

$$
\begin{aligned}
J_{33} &\simeq \frac{A}{a^3} + \frac{6Am_5x_5^2}{\sqrt{a^2+x_5^2}^5} - \sum_{i=1}^{6} \frac{Am_i}{|\lambda+Q_i|^3} \\
&= \frac{6Am_5x_5^2}{\sqrt{a^2+x_5^2}^5} + A\sum_{i=1}^{6} m_i \left(\frac{1}{a^3} - \frac{1}{|\lambda+Q_i|^3} \right) \\
&= A\Bigg(m_1 \frac{x_1[(a+x_1)^2+a(a+x_1)+a^2]}{a^3(a+x_1)^3} - m_1 \frac{x_1[(a-x_1)^2+a(a-x_1)+a^2]}{a^3(a-x_1)^3} \\
&\quad + 2m_3 \frac{(\sqrt{a^2+x_3^2}-a)[a^2+x_3^2+a\sqrt{a^2+x_3^2}+a^2]}{a^3\sqrt{a^2+x_3^2}^3} \\
&\quad + 2m_5 \frac{(\sqrt{a^2+x_5^2}-a)[a^2+x_5^2+a\sqrt{a^2+x_5^2}+a^2]}{a^3\sqrt{a^2+x_5^2}^3} + \frac{6m_5x_5^2}{\sqrt{a^2+x_5^2}^5} \Bigg).
\end{aligned}
\tag{B.8}
$$

It is now clear that the magnitude of J_{33} is at most A/a^4. Thus in order to have J_{33} large, a reasonable criterion for A is

$$
A \sim a^4. \tag{B.9}
$$

Next we check the third-order term in (B.7). The coefficient for s is approximately

$$
(1+4a^2)b^2 \simeq (1+4a^2)\frac{A}{a^3} \simeq \frac{4A}{a}, \tag{B.10}
$$

for large a. The choice of A in (B.9) makes this coefficient large which in turn implies there is a large eigenvalue. As a consequence, the condition number of the Jacobian matrix becomes large for large a, or large radius (with the size of molecule fixed). This illustrates that the problem of solving (6.1) is highly ill-conditioned. However, by using Theorem 6.1, this difficulty can be handled.

We next check the other constants in Theorem 6.1. By finding $\delta x \in \mathbb{R}^n$ such that

$$
F'(x_0)\delta x = F(x_0), \tag{B.11}
$$

the constant γ can be specified as

$$
\gamma = \|\delta x\|_\infty = \max\{\delta x_i,\ i = 1, \cdots, n\}. \tag{B.12}
$$

However, in solving (B.11) for δx, since $F'(x_0)$ is ill-conditioned, we need to use a robust algorithm. A method based on Singular-Value Decomposition (SVD) is chosen to deal with such difficulties.

The remaining constant α is the Lipschitz constant for F'. Since F' is continuously differentiable at $\lambda \neq 0$, we first find a bound on $\|F''\|$, where F'', a third-order tensor, is the derivative of F' with respect to (λ, Ω, β). Moreover, F'' can be represented as a linear operator from $\mathbb{R}^n$ to $\mathbb{R}^{n^2}$, which, in turn, can be expressed as an $(n^2 \times n)$ matrix P. It is easy to show that

$$\|F''\|_\infty \;\leq\; n \max\{P_{ij},\; i = 1, n^2,\; j = 1, n\}. \tag{B.13}$$

Because of the simplicity of this bound, the sup-norm is adopted in Theorem 6.1. Since in the Theorem, the constant α should be a Lipschitz constant on the whole domain D, we look for a symbolic representation of α. It can be checked that the elements in the matrix P have standard forms: 2λ, 2Ω, and

$$\begin{aligned}
&\sum_{i=1}^{4} \frac{-15Am_i\lambda_3^2}{|\lambda + Q_i|^7}(\lambda + Q_i) \;+\; \sum_{i=1}^{4} \frac{6Am_i\lambda_3}{|\lambda + Q_i|^5}\mathbf{e}_3 \;+\; \sum_{i=1}^{6} \frac{3Am_i}{|\lambda + Q_i|^5}(\lambda + Q_i) \\
&- \frac{15Am_5(\lambda_3 + x_5)^2}{|\lambda + Q_5|^7}(\lambda + Q_5) \;+\; \frac{6Am_5(\lambda_3 + x_5)}{|\lambda + Q_i|^5}\mathbf{e}_3 \\
&- \frac{15Am_6(\lambda_3 - x_6)^2}{|\lambda + Q_6|^7}(\lambda + Q_6) \;+\; \frac{6Am_6(\lambda_3 - x_6)}{|\lambda + Q_i|^5}\mathbf{e}_3,
\end{aligned}$$

where $\mathbf{e}_3 = (0\ 0\ 1)^T$. Let $m_{\max} = \max\{m_i,\; i = 1, \cdots, 6\}$. Bounds for these terms can be found to be

$$\{\; 2|\lambda|,\; 2|\Omega|,\; \frac{144Am_{\max}}{|\lambda|^4} \;\}. \tag{B.14}$$

In order to monitor the bound conveniently, we select A such that

$$\frac{144Am_{\max}}{|\lambda|^4} \;\leq\; 2|\lambda|,$$

which is equivalent to

$$A \;<\; \frac{|\lambda|^5}{72m_{\max}}. \tag{B.15}$$

This constraint on A associated with condition (B.9) provide us a good criterion to determine A such that the numerical method is tractable.

With (B.15) and (6.7), we can approximate $|\Omega|$ as

$$|\Omega| \simeq \left(\frac{A}{|\lambda|^3}\right)^{1/2} \leq \frac{|\lambda|}{\sqrt{72 m_{\max}}} \leq |\lambda|, \qquad (B.16)$$

since $m_{\max} \geq 1/6$. Thus (B.16) and (B.15) ensure that the maximum value in P is $2|\lambda|$. A symbolic bound of α can then be chosen to be

$$\alpha \simeq 2n|\lambda|. \qquad (B.17)$$

References

[1] BARKIN, Y.V., " 'Oblique' Regular Motions of a Satellite and Some Small Effects in the Motions of the Moon and Phobos," *Kosmicheskie Issledovaniya*, 23, 1 (1985), pp. 26–36.

[2] BELETSKII, V.V., *Motion of an Artificial Satellite about its Center of Mass*, Mechanics of Space Flight, Israel Program for Scientific Translations Ltd., 1966.

[3] CID, A. & R. ELIPE, "On the Motion of Three Rigid Bodies: Central Configurations," *Celestial Mechanics*, 37 (1985), pp. 113–126.

[4] DEPRIT, "A Note Concerning the TR-Transformation," *Celestial Mechanics*, 23, 4 (1981), pp. 299–305.

[5] DUBOSHIN, G.N., "Differential Equations of the Translational-Rotational Motion of Mutually Attracting Bodies," *Astronomicheskii Zhurnal*, 35, 2 (1958), pp. 265–276.

[6] DUBOSHIN, G.N., "On the Problem of Three Rigid Bodies," *Celestial Mechanics*, 33 (1984), pp. 31–47.

[7] ELIPE, R. & S. FERRER, "On the Equilibrium Solutions in the Circular Planar Restricted Three Rigid Bodies Problem," *Celestial Mechanics*, 37 (1985), pp. 59–70.

[8] GARCIA, C.B. & W.I. ZANGWILL, *Pathways to Solutions, Fixed Points, and Equilibria*, Prentice-Hall, 1981.

[9] HOLM, D., J.E. MARSDEN, T. RATIU & A. WEINSTEIN, "Nonlinear Stability of Fluid and Plasma Equilibria," *Physics Report*, 123 (1985), pp. 1–116.

[10] KELLOGG, B., *Numerical Methods*, University of Maryland, College Park, 1991, Class Notes.

[11] LIKINS, P.W. & R.E. ROBERSON, "Uniqueness of Equilibrium Attitudes for Earth-Pointing Satellites," *The Journal of the Astronautical Sciences*, XIII, 2 (1966), pp. 87–88.

[12] LONGMAN, R.W., P. HAGEDORN & A. BECK, "Stabilization Due to Gyroscopic Coupling in Dual-Spin Satellites Subject to Gravitational Torques," *Celestial Mechanics*, 25 (1981), pp. 353–373.

[13] MARSDEN, J.E. & T. RATIU, "Reduction of Poisson Manifolds," *Letters in Math. Phys.*, 11 (1986), pp. 161–169.

[14] MEIROVITCH, L., "On the Effect of Higher-order Inertia Integrals on the Attitude Stability of Earth-Pointing Satellites," *J. Astronautical Sciences*, 15, 1 (1968), pp. 14–18.

[15] MILLER, J.K. & T.C. DUXBURY, "The Phobos Gravity Field and Internal Properties," in *Television Investigations of Phobos*, G.A. AVANESOV, ed., October 1990.

[16] MILNOR, J., *Morse Theory*, Princeton University Press, 1963.

[17] ORTEGA, J.M., "The Newton-Kantorovich Theorem," *Am. Math. Monthly*, 75 (1968), pp. 658–660.

[18] ORTEGA, J.M. & W.C. RHEINBOLDT, *Iterative Solutions of Nonlinear Equations in Several Variables*, Academic Press, New York, 1970.

[19] PALAIS, R.S., "The Principle of Symmetric Criticality," *Comm. in Math. Physics*, 69, 1 (1979), pp. 19–30.

[20] RICE, J.R., *Numerical Methods, Software and Analysis*, McGraw-Hill, 1983.

[21] ROBERSON, R. E., "Circular Orbits of Non-infinitesimal Material Bodies in Inverse Square Fields," *The Journal of the Astronautical Sciences*, XV, II (1968), pp. 80–84.

[22] ROBERSON, R. E., "Stability of Orbiting Gyrostats in the Elementary Cases," *Ingenieur-Archive*, 39 (1970), pp. 317–329.

[23] RUMYANTSEV, V.V., "Dynamics and stability of rigid bodies," in *CIME Volume on Stereodynamics*, edizione cremonese, Roma, 1972, pp. 167–271.

[24] SARYCHEV, V.A., "Asymptotically Stable Rotational Motions of a Satellite," in *Peaceful Uses of Automation in Outer Space*, J.A. ASELTINE, ed., Plenum Press, 1966, Proceedings of the First IFAC Symposium on Automatic Control in the Peaceful Uses of Space, held June 1965 in Stavanger, Norway.

[25] SARYCHEV, V.A. & V.A. ZHTOUSTOV, *Periodic Oscillations of a Satellite in the Plane of an Elliptic Orbit*, Institute of Applied Mathematics (USSR), Moscow, 1975, No. 48, preprint.

[26] STEPANOV, S.Ia., "On the Steady Motions of a Gyrostat Satellite," *PMM*, 33, 1 (1969), pp. 127–131.

[27] WANG, L.-S., *Geometry, Dynamics and Control of Coupled Systems,* Ph.D. Dissertation, Electrical Engineering Department, University of Maryland, College Park, August, 1990.

[28] WANG, L.-S. & P.S. KRISHNAPRASAD, "Relative Equilibria of Two Rigid Bodies connected by a Ball-in-Socket Joint," *Proc. of the 1989 IEEE Conference on Decision and Control*, Tampa, FL (Dec. 1989), pp. 692–697.

[29] WANG, L.-S., P.S. KRISHNAPRASAD & J.H. MADDOCKS, "Hamiltonian Dynamics of a Rigid Body in a Central Gravitational Field," Systems Research Center, University of Maryland, College Park, TR-90-3, 1990, to appear in *Celestial Mechanics and Dynamical Astronomy*.

[30] WATSON, L.T., "Numerical Linear Algebra Aspects of Globally Convergent Homotopy Methods," *SIAM Review*, 28, 4 (December 1986), pp. 529–545.

[31] WITTENBURG, J. & L. LILOV, "Relative Equilibrium Positions and Their Stability for a Multi-body Satellite in a Circular Orbit," *Ingenieur-Archiv*, 44 (1975), pp. 269–279.